Fluid-induced anthropogenic and natural earthquake swarms are both driven by aseismic slip

Philippe Danré [1*], Louis De Barros [1], Frédéric Cappa [1,2], Jean-Paul Ampuero[1]

[1] Université Côte d'Azur, CNRS, Observatoire de la Côte d'Azur, IRD, Géoazur, France

[2] Institut Universitaire de France, Paris

Corresponding author: Philippe Danré (danre@geoazur.unice.fr)

Key Points:

- Scaling laws show that injection-induced and natural earthquake swarms have the same driving mechanism.
- Aseismic slip is a main driver of earthquake swarms, although its contribution differs from one swarm to another.
- We introduce a simple model based on fluid-induced aseismic slip propagation to relate observables to physical parameters.

Abstract

Anthropogenic fluid injections at depth induce seismicity which is generally organized as swarms, clustered in time and space, with moderate magnitudes. Earthquake swarms also occur in various geological contexts such as subduction zones, mountain ranges, volcanic and geothermal areas. While some similarities between anthropogenic and natural swarms have already been observed, whether they are driven by the same mechanism, or by different factors, is still an open question. Fluid pressure diffusion or aseismic deformation processes are often proposed to explain observations of hypocenters migration during swarms, while recent models suggest that swarm seismicity is rather triggered by fluid-induced aseismic fault slip. Here, using 22 natural and anthropogenic swarms, we observe that duration, migration velocity and total moment scale similarly for all swarms. This underlines a common driving process for both natural and induced swarms. These observations highlight the ubiquity of aseismic slip as main driver of earthquakes migration during swarms. After quantifying aseismic slip released during swarms, we propose an approach to estimate the seismic-to-total moment ratio, which we then compare to a theoretical estimation that depends on the migration velocity of the swarm, the effective stress drop and the velocity of the aseismic slip. Our findings lead to a generic explanation of earthquake swarms driving process.

Plain Language Summary

Earthquake swarms are a particular type of seismic activity, during which many earthquakes occur but with no mainshock distinguishable from the other events. They can be induced by anthropic hydraulic injections at depth, like during geothermal power exploitation and the massive storage of diverse fluids (i.e., wastewater, CO_2) in porous reservoir formations. Natural earthquake swarms are also observed in a large variety of geological contexts. Previous works showed that natural and injection-induced swarms share some similarities, like the migration of seismicity. But little is still known about their physics. Here, we explain the observed similarities in both types of swarms assuming that the earthquakes are triggered by the propagation of an aseismic slip transient, which in turn is induced by pressurized fluid circulation. We have reconciled a suite of independent observations made over different length and time scales, and our study provides a generic explanation of the driving process for the migration of earthquake swarms in the upper crust.

1. Introduction

Over the past 50 years, a number of studies have documented that fluid injection or extraction in subsurface reservoir formations can induce seismicity. These earthquakes can sometimes exceed magnitudes of 5 and have the potential to impact infrastructures and the public acceptance for geo-energy projects (Ellsworth, 2013; Keranen and Weingarten, 2018). The Rangely (US) experiment, conducted from 1969 to 1973, is one of the oldest and pioneering studies of seismicity caused by forced fluid injection (Raleigh et al., 1976). Another famous example is the 2006 Basel injection in Switzerland where 11.500 cubic meters of fluids were injected at about 5 km depth over the course of 6 days, leading to hundreds of earthquakes including a M_L=3.4 event just a few hours after the shut-in of the injection well was decided (Deichmann and Giardini, 2009). More generally, anthropogenic hydraulic injections are responsible for many seismic sequences, in association with geothermal heat reservoir development (Charléty et al., 2007; Albaric et al., 2014; Baisch et al., 2006; Kwiatek et al., 2019), hydraulic fracturing (Schultz et al., 2018), wastewater storage (Keranen et al., 2013), CO_2 sequestration (Zoback and Gorelick, 2012) or, at a smaller scale, during controlled fault activation experiments (Guglielmi et al., 2015). This fluid-induced seismic activity is singular as it organizes as a swarm with earthquakes clustered in time and space with no distinguishable mainshock/aftershock pattern.

Interestingly, earthquake swarms are also found in nature in a diversity of geological contexts such as mountain ranges (Jenatton et al., 2007), rift zones (De Barros et al., 2020), subduction zones (Metois et al., 2016), along transform faults (Roland and McGuire, 2009), or in geothermal and volcanic areas (Hensch et al., 2008; Shelly et al., 2013). Fluids are thought to play a key role in those natural swarms, either because seismicity is associated temporally or spatially with fluid circulation (Montgomery-Brown et al., 2019; Kraft et al., 2006; Shelly et al., 2013) or because they share similarities with injection-induced sequences (Skoumal et al., 2015). Indeed, the propagation of a seismicity front has been observed in sequences of anthropogenic origin (Goebel and Brodsky, 2018; Goebel et al., 2016) as well as in natural swarms (De Barros et al., 2020; Ross et al., 2020). This seismicity migration can be attributed to fluid pressure diffusion (Shapiro et al., 1997), aseismic slip (Roland and McGuire, 2009), or a combination of both (De Barros et al., 2021), as well as cascading events (Fischer and Hainzl, 2021). Studying the seismic moment released spatially during natural and injection-induced sequences also revealed they behave in a similar way (Fischer and Hainzl, 2017). However, despite those numerous observations, the drivers of seismicity in natural and induced swarms are still unkown.

The importance of aseismic slip during earthquake swarms is supported by several observations and models. Recently, based on hydromechanical modeling of fluid injection in a fault, studies showed that the increase of the critical earthquake nucleation size (the minimum size of a slip zone required for self-sustained seismic slip) with increasing fluid pressure leads to aseismic slip (Cappa et al., 2019), which may outpace the diffusing pressure front (Bhattacharya and Viesca, 2019; Larochelle et al., 2021) and may trigger seismicity near its edges where shear stresses increase (Wynants-Morel et al., 2020*)*. On the other hand, at first order, seismic moment is expected to scale with injected volume (McGarr, 2014). However, discrepancies to this scaling have been observed and can be explained by aseismic slip release (McGarr et Barbour, 2018*;* De Barros et al., 2019). This is in accordance with observations of aseismic slip using geodesy in the vicinity of a fluid injection site in the Brawley Basin (California) during an intense seismic swarm (Wei et al., 2015), with direct measurements of fault displacements during field injection experiments (Guglielmi et al., 2015), or indirectly by studying repeating earthquakes during the Soultz-Sous-Forêt (France) sequences associated with geothermal stimulation (Bourouis and Bernard, 2007; Lengliné et al., 2014). At the same time, natural swarms are also accompanied by aseismic slip release, as revealed by geodesy and slip inversions (Lohman and McGuire, 2007; Gualandi et al., 2017), or by studying dual velocity migrations and repeating earthquakes like during the 2015 swarm in the Gulf of Corinth (Greece) (De Barros et al., 2020). However, geodetic observations of aseismic slip associated with earthquake swarms remain rare and difficult to achieve, given the depth and low deformation rate of such sequences. Thus, important questions on the contribution of aseismic slip during swarm activity remain.

In this study, we aim at exploring if injection-induced seismic sequences and natural swarms may be explained by the same processes. We first explore the similarities between both types of swarms, which then allows us to introduce a simple but realistic framework to constrain the aseismic slip released. We finally propose a physical model, based on observations, in which both types of swarms are driven by aseismic slip, which in turn is triggered by a fluid pressure perturbation.

2. Natural and injection-induced catalogs

To explain the similarities between natural and injection-induced swarms, as well as their most remarkable features, we focus on a global dataset of 22 earthquake swarms, from either injection-induced or natural origin. For natural earthquake sequences, we focus on swarms in which fluid processes have been previously discussed. For example, we do not consider the swarm studied by Lohman and McGuire (2007) which is interpreted as driven solely by a slow slip event. Likewise, we do not consider swarms taking place near volcanoes or in subduction zones as they might involve different processes (Roman and Cashman, 2006). For simplicity, the injection-induced sequences studied here are limited to sites where there is only one main injection well and to swarms that present a simple geometry. The earthquake catalogs used are described in detail in the Supplementary materials (Text S2), but we present them briefly below (Figure 1).

The 8 natural swarms have diverse geological contexts. For instance, the 2003-2004 Ubaye (hereafter, named UBY) sequence (Jenatton et al., 2007) occurred in a near-zero strain-rate area in the southern French Alps, lasted ~2 years and comprised thousands of events (Daniel et al., 2011), while the 2014 Crevoux swarm lasted only one week and produced ~270 seismic events. The 2001 and 2015 Corinth (CRT) swarms (Duverger et al., 2018; De Barros et al., 2020) took place in a very fast extensional (~15 mm/year) rift zone in Greece with maximum magnitudes of $M_w = 3.8$ and $M_w = 2.5$, respectively. In California, a $M_w = 4.4$ earthquake occurred during the Cahuilla swarm (Ross et al., 2020), which lasted more than 4 years (CHA). Three swarms (SW2 in 2001, SW4 in 2008 and SW6 in 2013) along the Húsavík–Flatey fault system in Iceland are also considered in this study (Passarelli et al., 2018).

Most of the 14 injection-induced swarms we consider originate from geothermal exploitation. However, they span a wide range of characteristics, including the injected fluid volume and the injection depth. The Soultz-sous-Forêts (SZ) stimulations took place in 1993, 1995, 1996, 2000, 2003, and 2004 in Eastern France during a tenth of days, with injected volumes up to 37,000 m^3 along several distinct wells, each time inducing a prolific seismic response with hundreds of events or more (Bourouis and Bernard, 2007; Gerard et al., 1997; Cuenot et al., 2008; Calo and Dorbath, 2013; Dyer et al., 2004). Just nearby, the Rittershoffen seismic sequences were induced also by a hydraulic stimulation (Lengliné et al., 2017). The Paralana, Cooper Basin 2003 and 2012 injections (PAR, CB03, CB12) took place in Australia, and also exhibited an intense seismic activity associated with fluid injection (Albaric et al., 2014; Baisch et al., 2006; Baisch et al., 2015). Recently, the ST1 sequence in Finland corresponds to a control experiment aiming at mitigating the seismicity induced by fluid injection. In this case, 18,000

m^3 of fluids were injected during 49 days, leading to hundreds of events but successfully preventing the occurrence of earthquakes of magnitude greater than 2.0 (Kwiatek et al., 2019). Finally, the Paradox Valley swarm (PRX) is induced by wastewater disposal, with several millions cubic meters of fluids injected since 1985 leading to a long-lasting earthquake activity with several events of magnitudes $M_w>4$ (Ake et al., 2005).

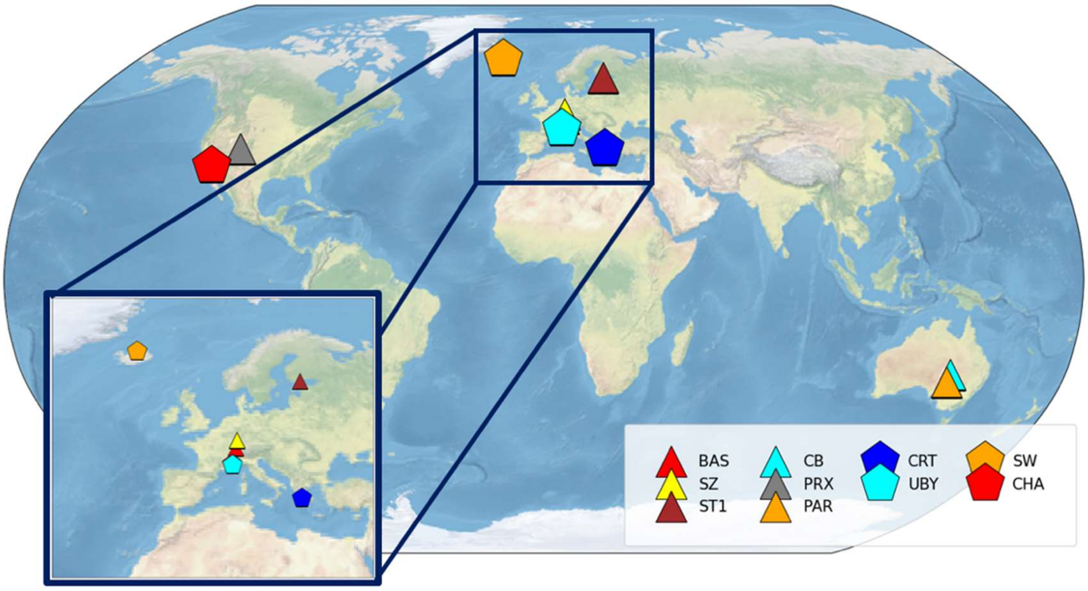

Figure 1. World map of the location of studied seismic sequences. Pentagons indicate natural swarms while triangles indicate injection-induced ones. BAS : Basel; SZ : Soultz-sous-Forêts; CB : Cooper Basin; PRX : Paradox Valley; PAR : Paralana; CRT : Gulf of Corinth; UBY : Ubaye ; CHA : Cahuilla.

3. Methods

3.1 Migration velocity

The average migration velocity of each swarm is estimated by fitting the seismicity front with a linear model. The spatial origin of the swarm is chosen as the median of the hypocentral coordinates of the 10 first events. The origin time is defined as the time of the first event. Migration duration is defined as the time during which the envelope of distance to the spatial origin increases continuously. We compute the seismicity front as the 90th percentile of event distances in a sliding window containing 50 events (Figure 2). Seismicity fronts have been modelled by either a diffusive law, constant speed or more complex relationships (Goebel and Brodsky, 2018; De Barros et al., 2021). However, here, the shape of the migration is not investigated, as we only focus on estimating an average migration velocity, in order to make first-order comparisons among swarms. We fit a linear model over the seismicity front during the migration period of each sequence, leading to consistent and similar r^2 values compared to other classical migration models like pressure diffusion (Supplementary Figures S1 and S2). This procedure yields an average migration velocity for each sequence. The complete migration fits can be found in the Supplementary materials.

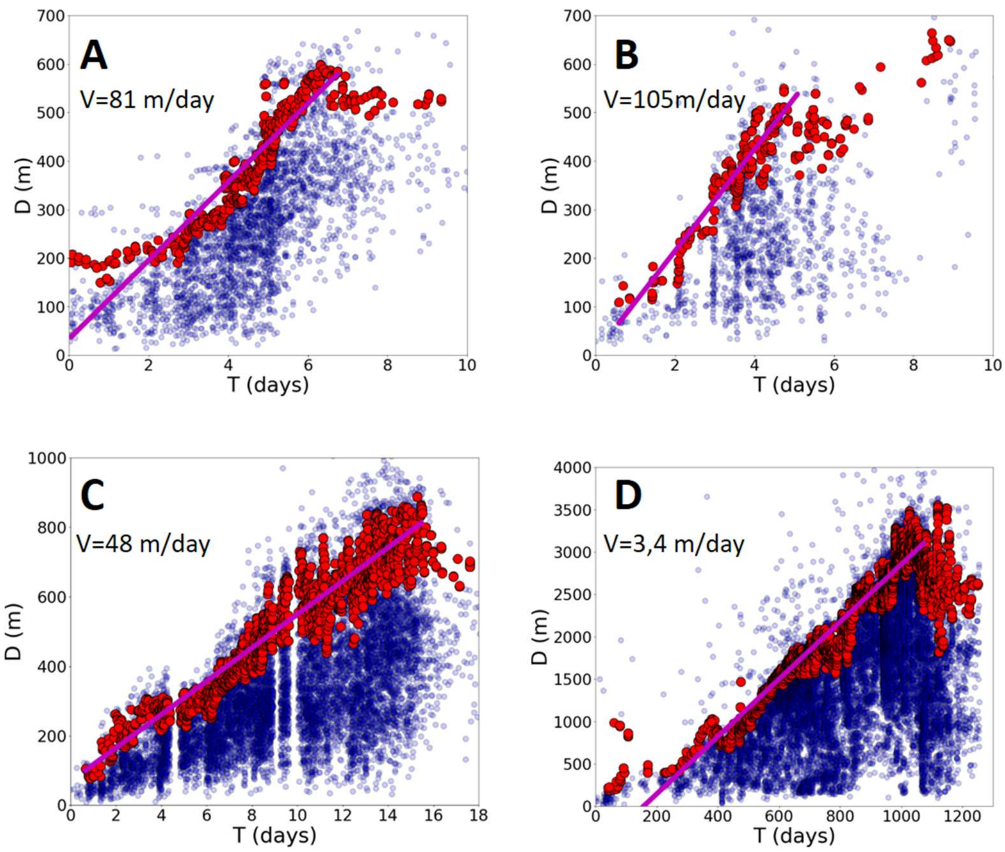

Figure 2. Distance-time plot of seismicity and average migration speed estimates for (A) Basel, (B) Corinth, (C) Soultz-Sous-Forêts 1993, and (D) Cahuilla. Blue points indicate, for each event, the distance to the origin (m) and ocurrence time (days). Red circles correspond to the seismicity front. Magenta line is the linear best-fit made over the seismicity front during the migration period. For the other swarms, see the Supplementary materials (Figures S1 and S2).

3.2 Effective stress drop

Following the approach of Fischer and Hainzl (2017), the seismicity area is computed by fitting a 2D plane over the 3D distribution of hypocenters, after removing the few outliers in the catalogs but not in the swarm area. Hypocenters are then projected over the plane, and a convex hull is fitted to delineate and return the seismicity area S. We then compute the radius of the seismicity area, assuming it is circular at first order, with $\boldsymbol{R} = \sqrt{\boldsymbol{S}/\boldsymbol{\pi}}$.

By analogy with the moment-size relationship for circular ruptures, the effective stress drop of a swarm is defined as (Fischer and Hainzl, 2017):

$$\boldsymbol{\Delta\sigma_e} = \frac{\boldsymbol{7M_{0,seismic}}}{\boldsymbol{16R^3}} \quad (1)$$

where $\boldsymbol{M_{0,seismic}}$ is the cumulative seismic moment during the swarm. A low effective stress drop suggests seismic asperities are far apart, whereas values close to earthquake stress drops, typically around 1-100 MPa (Cocco et al., 2016), suggest that seismic asperities cover most of the slipping area. The former has been proposed to indicate a large contribution of aseismic slip during swarms (Fischer and Hainzl, 2017).

3.3 Total moment estimation

The total moment is defined as the sum of the seismic and aseismic moments. Aseismic slip quantification is difficult for injection-induced sequences because the associated deformations are small and extend over long durations, leading to small strain rates that are hard to observe. The same issue affects natural swarms, in addition to the instrumental limitations, the distance between sensors and the source depth. For instance, during the Icelandic swarms, despite the substantial aseismic slip expected, no corresponding signal was detected on the neighboring GPS stations (Passarelli et al., 2018).

We propose a simple way to estimate, roughly, the amount of aseismic slip in a swarm in the absence of geodetic data. Studies of slow slip transients in subduction zones and on creeping faults have shown that the cumulative slip of repeating earthquake sequences equals the surrounding aseismic slip (Matsuzawa et al., 2004; Uchida, 2019). Based on recent works demonstrating that the migration front of seismicity can be directly triggered by the shear stress perturbation induced by aseismic slip (Cappa et al., 2019; Wynants-Morel et al., 2020; Figure 3), we make an analogy with slow slip transients. We suppose that the slip released seismically over discrete asperities equals the surrounding aseismic slip. We neglect the contribution of afterslip given that it represents only ~20% of the slip occurring over the seismically slipping area for simulations of small repeating earthquakes (Chen et Lapusta, 2009). Assuming that the asperity associated with the largest earthquake in the swarm only ruptures once, its slip gives an order of magnitude of the slip over the whole area. For each sequence, we isolate the largest event, with moment $\boldsymbol{M_{0,max} = G\, D_{max}\, \pi R_{max}^2}$, assuming a circular rupture of radius $\boldsymbol{R_{max}}$, a shear modulus G=30GPa (a conventional value for crustal rocks) and a static stress drop $\boldsymbol{\Delta\sigma_{max} = \frac{7\, M_{0,max}}{16\, R_{max}^3}}$ (Madariaga, 1976) of 10 MPa (unless a more precise value is provided in the literature, see Supplementary Materials), in order to compute the slip $\boldsymbol{D_{max}}$ over this asperity as (Madariaga, 1976):

$$\boldsymbol{D_{max} = M_{0,max}^{1/3}\, \frac{(16\Delta\sigma_{max})^{2/3}}{G\pi 7^{2/3}}} \qquad (2)$$

Given that seismic moment is released over brittle asperities and aseismic slip is released in between them, we estimate the total moment over the seismicity area as:

$$\boldsymbol{M_{0,total} = G\, D_{max} S} \qquad (3)$$

While the effective stress drop qualitatively indicates the importance of aseismic slip during a swarm, the rough quantification approach proposed here allows us to better constrain aseismic moment release for each sequence.

3.4 Seismic to total moment ratio

By considering the total (seismic and aseismic) slip is equivalent to a single slip event over a circular area of radius R and stress drop $\boldsymbol{\Delta\sigma_{total}}$ (Figure 3), we have (Madariaga, 1976):

$$\boldsymbol{M_{0,total} = \frac{16}{7}\Delta\sigma_{total}R^3} \tag{4}$$

The rupture velocity of a slow slip event is related to its stress drop and to its maximum slip velocity $\boldsymbol{V_{max}}$ by (Ampuero and Rubin, 2008; Rubin, 2008; Passelègue et al., 2020):

$$\boldsymbol{V_{rupt} = \frac{G\,V_{max}}{n\,\Delta\sigma_{total}}} \tag{5}$$

where $\boldsymbol{n}$ is the ratio between the strength drop (peak minus residual stress) and the stress drop, $\boldsymbol{\Delta\sigma_{total}}$ (initial minus residual stress). In several numerical simulations of slow slip, n~10 (Hawthorne and Rubin, 2013; Lambert et al., 2021).

We hypothesize that seismicity is triggered by fluid-induced aseismic slip. Therefore, the seismicity front follows the aseismic slip front (Bhattacharya and Viesca, 2019; Wynants-Morel et al., 2020; De Barros et al., 2021) like observed with tectonic tremors migration and slow slip propagation in subduction zones (Bartlow et al., 2011). The migration velocity of the swarms is then equal to the rupture velocity of the aseismic slip ($V_{rupt} = V_{migr}$). Our hypothesis and the previously discussed observations are summarized in Figure 3. Combining Equations 4 and 5 we then have:

$$\boldsymbol{M_{0,total} = \frac{16}{7}\,\frac{G\,V_{max}}{n\,V_{migr}}R^3} \tag{6}$$

This leads us to the following expression for the ratio *r* of seismic to total moment:

$$\boldsymbol{r = \frac{M_{0,seismic}}{M_{0,total}} = \frac{7\,M_{0,seismic}}{16\,R^3}\frac{n\,V_{migr}}{G\,V_{max}}} \tag{7}$$

This equation can be written in a more compact form using the effective stress drop (Equation 1):

$$\boldsymbol{r = \frac{n\, \Delta\sigma_e\, V_{migr}}{G\, V_{max}}} \tag{8}$$

This relation links the ratio of the cumulative seismic moment to total moment to the product of the migration velocity and the effective stress drop of the swarm.

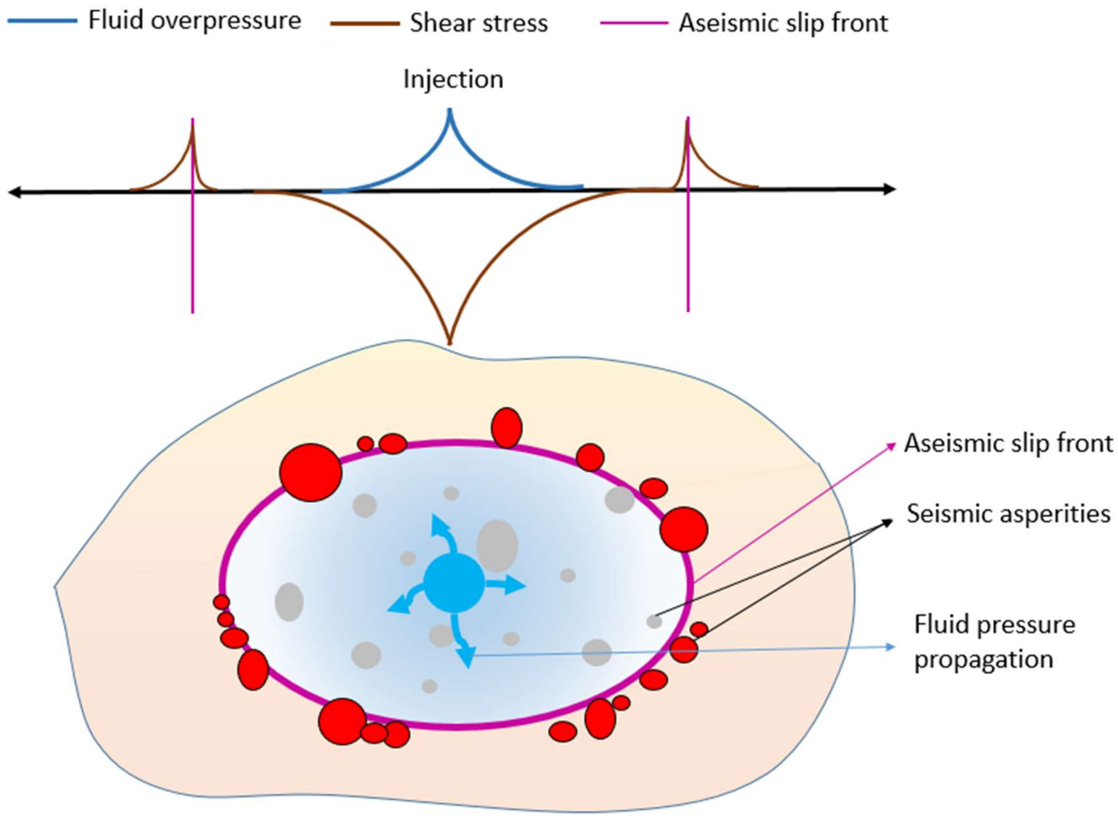

Figure 3. Schematic view of the model considered here, based on observations and hypothesis that depicts simplistically the processes occurring during swarm propagation. Aseismic slip front (purple) propagation leads to shear stress concentration at its tips (brown), triggering seismicity on asperities (red patches), which correspond to the seismicity front. Seismicity is also triggered within the slipping zone (grey patches).

4. Results

4.1 Aseismic slip drives natural and induced swarms

The estimated velocities of the 22 swarms studied here range from a few meters per day, like for the Cahuilla swarm (Ross et al., 2020), to more than 1 km/day, like for the Rittershoffen sequence (Lengliné et al., 2017). Figure 4 shows the migration velocity V as a function of swarm duration T, for induced and natural swarms. We included velocity measurements from the literature for additional cases (Kim et al., 2013; Seeber et al., 2004; Duverger et al., 2015; Yoshida et al., 2018; Duboeuf, 2018). For the sake of comparison, we also show the migration velocity of slow slip events in subduction zones (Gao et al., 2012). For these events, velocities correspond to the propagation of aseismic slip, which is characterized either with geodesy (Schmidt and Gao, 2010) or with tremor migration (Bartlow et al., 2011; Ito et al., 2007).

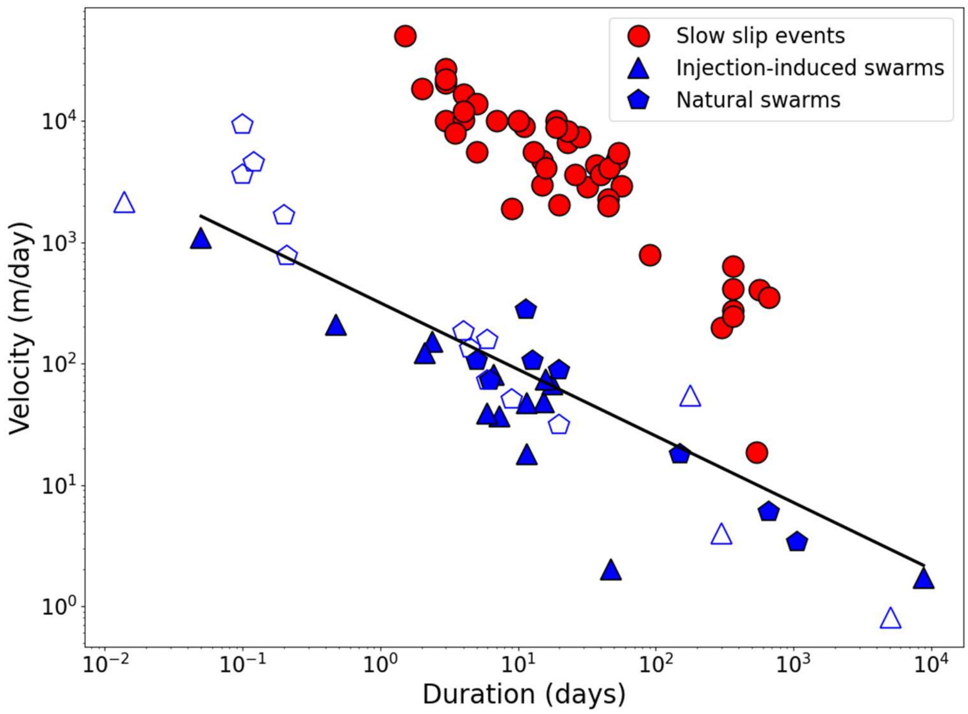

Figure 4. Scaling of propagation velocity with duration for swarms and slow slip events (SSEs). Red dots represent SSE data from (Gao et al., 2012). Filled triangles and pentagons represent injection-induced and natural swarms, respectively, for which we determined migration velocity and duration based on seismicity catalogs. Empty symbols represent migration velocities and durations directly taken from the literature (Kim et al., 2013; Seeber et al., 2004; Duverger et al., 2015; Yoshida et al., 2018; Duboeuf, 2018). Black line represents the best-fitting power-law relation between velocities and durations of natural and induced swarms ($R^2 = 0.76$).

Two main observations can be made. First, injection-induced and natural swarms follow the same scaling $\boldsymbol{V \alpha\, T^{-\gamma}}$, with $\boldsymbol{\gamma = 0.6}$ and $\boldsymbol{\gamma = 0.7}$ for each swarm subset, respectively. In addition to the other similarities discussed beforehand, the continuous scaling of velocity with duration for all swarms is direct evidence that both types of sequences, natural and injection-induced, obey the same physics for all velocity ranges (from a few meters per day in the Ubaye and Cahuilla years-long sequences, to ~1100 m/day for Rittershoffen which barely lasts a day). As anthropogenic seismicity is induced (though indirectly) by fluid injection (Bentz et al., 2020), this similar scaling suggests that natural swarms studied here are also a consequence of fluid pressure perturbations.

Second, the velocity-duration scaling is similar for swarms ($\boldsymbol{V \alpha\, T^{-0.55}}$) and for the SSEs ($\boldsymbol{V \alpha\, T^{-0.5}}$) reported by Gao et al. (2012), despite higher velocities for the latter, typically around 1 to 10 km/day. The small difference of scaling exponents can be explained by different velocity measurements methods for swarms and SSEs. The scaling similarity indicates that the migration of swarms globally behaves like the propagation of aseismic slip, supporting our assumption that $V_{rupt} = V_{migr}$. The observed scaling for swarms, $\boldsymbol{V \alpha\, T^{-0.55}}$, is compatible with fluid pressure diffusion. However, a similar scaling is obtained for SSEs, which exhibit individual linear migrations (Houston et al., 2011) and are not directly driven by fluid diffusion. Other mechanisms have been proposed to explain such scaling for SSEs, like a uniform stress drop or a uniform slip over the ruptured area (Ide et al., 2007). These mechanisms might also be valid for swarms, explaining then the observed continuum of characteristics (Figure 4). Therefore, a general scaling compatible with diffusion does not imply that individual swarms are directly driven by fluid diffusion, but its similarity with SSE scaling suggests that swarm migration velocity behaves like an aseismic slip migration velocity.

The effective stress drop $\boldsymbol{\Delta\sigma_e}$ for the swarms studied is found to range between 1 kPa and 1 MPa (Figure 5). Those values are lower than typical values of static stress drop for earthquakes, which usually range between 1 and 100 MPa (Cocco et al., 2016), and are more similar to the stress drop values of SSEs (Brodsky and Mori, 2007). Thus, $\boldsymbol{\Delta\sigma_e}$ values may indicate an aseismic component in the swarm processes. For instance, $\boldsymbol{\Delta\sigma_e}$ = 1 kPa for the Soultz-sous-Forêt stimulations (1993, 1995, 1996) could suggest an important aseismic moment release, while $\boldsymbol{\Delta\sigma_e}$ = 1 MPa for the Basel injection might mean that aseismic slip is relatively less important in this case. $\boldsymbol{\Delta\sigma_e}$ ranges are similar for natural and injection-induced sequences (Figure 5), indicating once again similar processes for both.

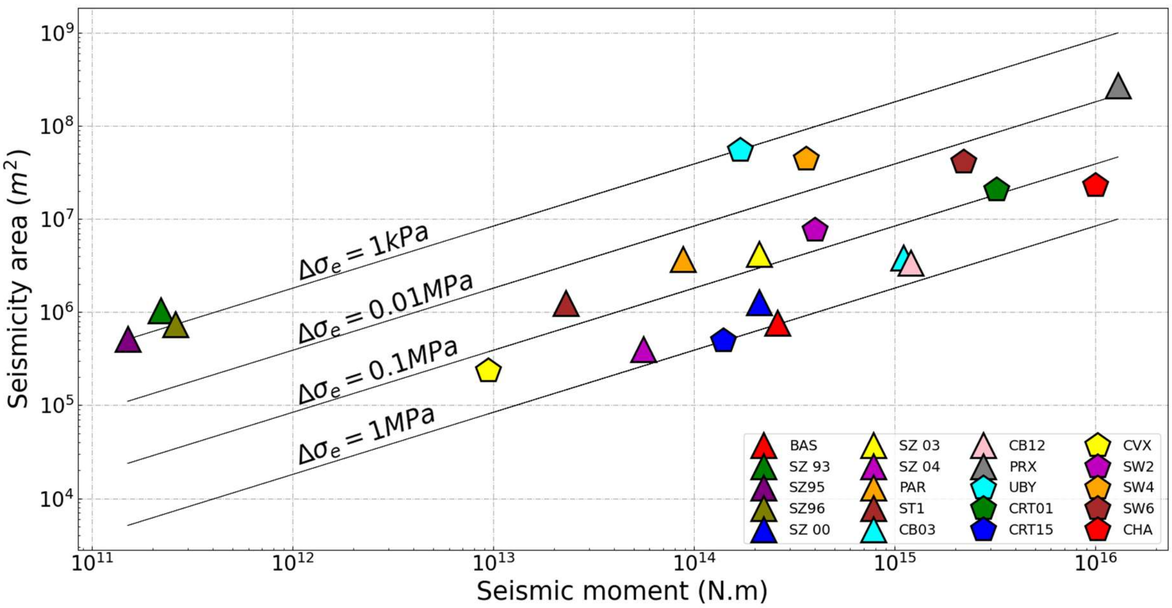

Figure 5. Seismicity area (m²) as a function of the cumulative seismic moment released during 20 of the swarms studied here (the two Rittershoffen sequences had no seismic moment available so they are not represented here). Triangles correspond to injection-induced sequences while pentagons refer to natural swarms. Black lines represent different values of the effective stress drop $\boldsymbol{\Delta\sigma_e}$.

Based on similar velocity-duration scaling and effective stress drop values, natural and injection-induced swarms appear to share the same driving processes, in which aseismic slip seems ubiquitous, like depicted on Figure 3. The seismicity front delineates the aseismic slip rupture front and the seismicity area corresponds to the aseismic slip area, in a similar way as tremors locations in SSEs zones delineate slip migration and area (Bartlow et al., 2011). However, as suggested by the variability of $\boldsymbol{\Delta\sigma_e}$ values, the aseismic contribution might be different from one swarm to another.

4.2 Aseismic contribution differs among swarms

Once the total moment $\boldsymbol{M_{0,total}}$ for each swarm is computed (Equations 2 and 3), we compare it to the seismic moment released by using the seismic to total moment ratio *r*. A value of *r* close to 1 indicates that moment release is mainly seismic, while a low value shows that moment release is significantly aseismic. As shown in Figure 6a, *r* ranges from 0.001 to almost 1. For the Basel injection-induced sequence, $r = 0.97$, suggesting that aseismic deformation is low in this case, while for the Ubaye natural swarm, r = 0.005, indicating an important aseismic moment release.

For the Soultz 1993 sequence, despite an injected fluid volume of the same order of magnitude as in the Basel injection (Deichmann and Giardini, 2009), the cumulative seismic moment is 3 orders of magnitude lower than the Basel one. This can be explained by an important aseismic moment release (r ~ 0.001) during the Soultz sequence. Therefore, our computations seem to validate that the strong difference of seismic moment release for similar injected volumes observed for injection-induced earthquake swarms can simply reflect the amount of induced aseismic deformation (McGarr and Barbour, 2018; De Barros et al., 2019).

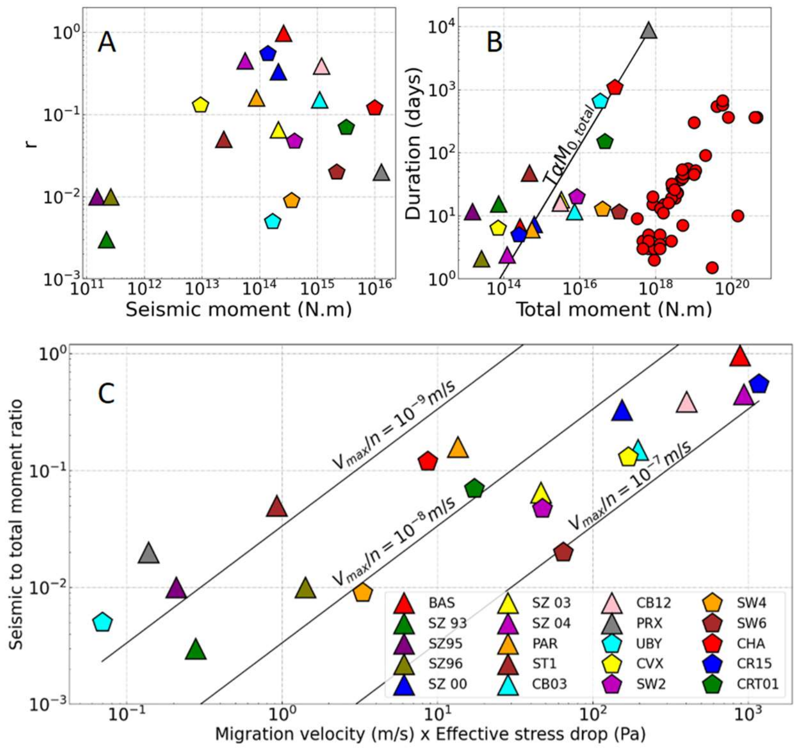

Figure 6. (**A**) Seismic to total moment ratio, as a function of the seismic moment released during each swarm, for the sequences studied here. (**B**) Duration as a function of the estimated total moment. Black line represents the 1:1 scaling. Red dots correspond to the SSE data from Gao et al. (2012). (**C**) Seismic to total moment ratio for the swarms studied here, as a function of the product of the migration velocity and the effective stress drop. The black lines correspond to different values of $\frac{V_{max}}{n}$, assuming G = 30 GPa (see Equation 8).

Interestingly, one can also note that the scaling of duration with estimated total moment (Figure 6b) seems to be close to 1:1, similarly to the scaling between event duration and aseismic moment observed for SSEs (Ide et al., 2007; Peng and Gomberg, 2010). This correlation is quite weak, but seismic moment versus duration does not exhibit such a scaling (Passarelli et al., 2018). Our total moment estimate accounts for the “hidden” aseismic slip release occuring during swarms : in the compilation of duration versus moment observations by Peng and Gomberg (2010), many swarms have much longer duration than expected for slow slip events whose aseismic moment equals the swarm's cumulative seismic moment. This difference can be explained if the aseismic moment contribution in swarms, which has not been accounted for, is significant.

Using Equation 8, we can relate the seismic to total moment ratio to two observables, the effective stress drop and migration velocity (see Figure 6c). We estimate $\boldsymbol{V_{max}/n}$ being between $\mathbf{10^{-10}}$ and $\mathbf{10^{-7}}$ m/s, which corresponds to $\boldsymbol{V_{max}}$ values consistent with expected orders of magnitudes (Roland and McGuire, 2009; Glowacka et al., 2001) if we consider a value of n~10 (Hawthorne and Rubin, 2013; Lambert et al., 2021). Variability in $\boldsymbol{V_{max}}$ explains why the observed scaling between $\boldsymbol{r}$ and $\boldsymbol{\Delta\sigma_e * V_{migr}}$ is not as linear as expected. As the general trend shows a scaling different than the isovalues of V_{max}/n, it means that V_{max} also depends, through fault and stress properties, on the seismic-to-total seismic ratio.

5. Discussion and conclusions

In addition to the numerous observations in the literature made on the similarities between natural and injection-induced earthquake swarms, our global analysis of both types of sequences helps to better understand the processes taking place during those phenomena. Indeed, based on the velocity versus duration scaling continuity, the drivers of natural and anthropogenic swarms appear to be the same. Aseismic slip is a solid candidate to explain seismicity propagation, as it has already been observed for particular sequences of both types, but also as the scaling of migration velocity versus duration of swarms is similar to that of slow slip events (Figure 4). This is of particular interest given that for anthropogenic sequences aseismic slip is thought to have a significant importance in the relation between moment and injected fluid volume, on which anticipation of the seismic moment released is often based

(McGarr and Barbour, 2018; De Barros et al., 2019). Therefore, it appears that the role of aseismic slip is not limited to slip release but might be responsible for the dynamics of swarms, through shear stress transfer at its tips triggering a migrating seismicity (Figure 3). Such a stress transfer originating from an aseismic slip zone and seismicity triggering has been observed in different contexts like in the Boso Peninsula in Japan where two SSEs lead to two earthquake swarms at their tips (Hirose et al., 2014).

As mentioned above, our migration velocity measurements return us average velocities, but some information might be left out. De Barros et al. (2021) indeed showed that seismic fronts have a complex time-dependent shape, revealing the seismogenic state of faults. However, we still get reliable results depicting the behavior of swarms, not on an individual but on a global scale.

If aseismic slip provides an explanation for the observations on swarms, making parallels with existing aseismic transients gives more information on its importance. Using observations made on repeating earthquake sequences, we were able to compute total (and therefore aseismic) moment released during swarms. While our quantification of total moment is rough and relies on several simplifying assumptions, we hope that further systematic study of relevant parameters like stress drop will help confirm our findings. Still, our results indicate that the importance of aseismic slip differs among swarms; even though it always drives seismicity, it can sometimes represent a small fraction of the deformation (like for the Basel case) or actually be the main slip mode (like for the Soultz 1993 sequence). Our approach overcomes the difficulties caused by the low and long deformations occurring during those sequences, preventing geodetic observations in most cases.

Based on the studies of slow slip events, we introduced a simple mechanical model to relate different observables (Equation 8). This allows to give a physical sense to their measurements and provides a first order physical approach to the slip dynamics during swarms. Further work on earthquake swarms might help identifying or better constraining the relevant parameters to model and understand in detail swarm dynamics.

Here, we also show that the slip velocity, together with the migration velocity and the effective stress drop, are the crucial parameters to characterize the seismic and aseismic moment partitioning in swarms. Among other properties, these three parameters depend on the stress state and on the proximity of the fault to failure (Hainzl and Fischer, 2002; Fischer and Hainzl, 2017; Passelègue et al., 2020; Wynants-Morel et al., 2020; De Barros et al., 2021). These relationships therefore deserve to be investigated in order to anticipate the swarm evolution, especially given that similarities are found between swarms and foreshock sequences of some major earthquakes (Chen and Shearer, 2013).

We here worked on catalogs selected for their simplicity (simple injection history and geometry) and removed from the analysis swarms from different contexts (e.g., subduction, volcanoes). However, we have reconciled observations made since decades on the two types of swarms, injection-induced and natural, by proposing a realistic scenario involving aseismic slip triggering seismicity, based on multiple observations made on 22 sequences. This opens interesting perspectives to better understand seismic swarms, their propagation, and improve their monitoring in order to anticipate potential large earthquakes. It also paves a way to studying natural and injection-induced swarms as the same phenomena.

Acknowledgments

Data for the Iceland swarms were kindly made available by the Icelandic Meteorological Office (SIL, https://en.vedur.is/) and L. Passarelli (Passarelli et al., 2018). Data from the Paralana sequence and from the Ubaye swarm were made available by J. Albaric (Albaric et al., 2014) and G. Daniel (Daniel et al., 2011) respectively. Catalog for the Cahuilla swarm were provided

by Z. Ross and D. Trugman (Ross et al., 2020). Data for the Soultz fluid injections are available on the CDGP web services (https://cdgp.u-strasbg.fr/). Data for the Cooper Basin injections are available on the EPOS platform (https://tcs.ah-epos.eu/). Data for the Paradox Valley fluid injection are available on the US Bureau of Reclamation (https://www.usbr.gov/uc/progact/paradox/index.html). Rittershoffen data was made available by O. Lengliné (Lengliné et al., 2017).

References

Ake, J., Mahrer, K., O'Connell, D., & Block, L. (2005). Deep-injection and closely monitored induced seismicity at Paradox Valley, Colorado. *Bulletin of the Seismological Society of America*, *95*(2), 664-683.

Albaric, J., Oye, V., Langet, N., Hasting, M., Lecomte, I., Iranpour, K., ... & Reid, P. (2014). Monitoring of induced seismicity during the first geothermal reservoir stimulation at Paralana, Australia. *Geothermics*, *52*, 120-131.

Ampuero, J. P., & Rubin, A. M. (2008). Earthquake nucleation on rate and state faults–Aging and slip laws. *Journal of Geophysical Research: Solid Earth*, *113*(B1).

Baisch, S., Weidler, R., Vörös, R., Wyborn, D., & de Graaf, L. (2006). Induced seismicity during the stimulation of a geothermal HFR reservoir in the Cooper Basin, Australia. *Bulletin of the Seismological Society of America*, *96*(6), 2242-2256.

Baisch, Stefan and Rothert, Elmar and Stang, Henrik and Vörös, Robert and Koch, Christopher and McMahon, Andrew (2015) *Continued Geothermal Reservoir Stimulation Experiments in the Cooper Basin (Australia).* Bulletin of the Seismological Society of America, 105 (1). pp. 198-209

Bartlow, Noel M., et al. "Space-time correlation of slip and tremor during the 2009 Cascadia slow slip event." *Geophysical Research Letters* 38.18 (2011).

Bentz, S., Kwiatek, G., Martínez-Garzón, P., Bohnhoff, M., & Dresen, G. (2020). Seismic moment evolution during hydraulic stimulations. *Geophysical Research Letters*, *47*(5), e2019GL086185.

Bhattacharya, P., & Viesca, R. C. (2019). Fluid-induced aseismic fault slip outpaces pore-fluid migration. *Science*, *364*(6439), 464-468.

Bourouis, S., & Bernard, P. (2007). Evidence for coupled seismic and aseismic fault slip during water injection in the geothermal site of Soultz (France), and implications for seismogenic transients. *Geophysical Journal International*, *169*(2), 723-732.

Brodsky, E. E., & Mori, J. (2007). Creep events slip less than ordinary earthquakes. *Geophysical Research Letters*, *34*(16).

Calò, M., & Dorbath, C. (2013). Different behaviours of the seismic velocity field at Soultz-sous-Forêts revealed by 4-D seismic tomography: case study of GPK3 and GPK2 injection tests. *Geophysical Journal International*, *194*(2), 1119-1137.

Cappa, F., Scuderi, M. M., Collettini, C., Guglielmi, Y., & Avouac, J. P. (2019). Stabilization of fault slip by fluid injection in the laboratory and in situ, Sci.

Charléty, J., Cuenot, N., Dorbath, L., Dorbath, C., Haessler, H., & Frogneux, M. (2007). Large earthquakes during hydraulic stimulations at the geothermal site of Soultz-sous-Forêts. *International Journal of Rock Mechanics and Mining Sciences*, *44*(8), 1091-1105.

Chen, T., & Lapusta, N. (2009). Scaling of small repeating earthquakes explained by interaction of seismic and aseismic slip in a rate and state fault model. *Journal of Geophysical Research: Solid Earth*, *114*(B1).

Chen, X., & Shearer, P. M. (2013). California foreshock sequences suggest aseismic triggering process. *Geophysical Research Letters*, *40*(11), 2602-2607.

Cocco, M., Tinti, E., & Cirella, A. (2016). On the scale dependence of earthquake stress drop. *Journal of Seismology*, *20*(4), 1151-1170.

Cuenot, N., Dorbath, C., & Dorbath, L. (2008). Analysis of the microseismicity induced by fluid injections at the EGS site of Soultz-sous-Forêts (Alsace, France): implications for the characterization of the geothermal reservoir properties. *Pure and Applied Geophysics*, *165*(5), 797-828.

Daniel, G., et al. (2011), Changes in effective stress during the 2003–2004 Ubaye seismic swarm, France, *J. Geophys. Res.*, 116, B01309

De Barros, L., Cappa, F., Guglielmi, Y., Duboeuf, L., & Grasso, J. R. (2019). Energy of injection-induced seismicity predicted from in-situ experiments. *Scientific reports*, *9*(1), 1-11.

De Barros, L., Cappa, F., Deschamps, A., & Dublanchet, P. (2020). Imbricated aseismic slip and fluid diffusion drive a seismic swarm in the Corinth Gulf, Greece. *Geophysical Research Letters*, *47*(9), e2020GL087142.

De Barros, L., Wynants-Morel, N., Cappa, F., & Danré, P. (2021). Migration of fluid-induced seismicity reveals the seismogenic state of faults. *Journal of Geophysical Research: Solid Earth*, 126, e2021JB022767.

Deichmann, N., & Giardini, D. (2009). Earthquakes induced by the stimulation of an enhanced geothermal system below Basel (Switzerland). *Seismological Research Letters*, *80*(5), 784-798.

Duboeuf, L. (2018). *Injections de fluide dans une zone de faille (LSBB, Rustrel): sismicité induite et déformation asismique* (Doctoral dissertation, Université Côte d'Azur).

Duverger, C., Godano, M., Bernard, P., Lyon-Caen, H., & Lambotte, S. (2015). The 2003–2004 seismic swarm in the western Corinth rift: Evidence for a multiscale pore pressure diffusion process along a permeable fault system. *Geophysical Research Letters*, *42*(18), 7374-7382.

Duverger, C., Lambotte, S., Bernard, P., Lyon-Caen, H., Deschamps, A., & Nercessian, A. (2018). Dynamics of microseismicity and its relationship with the active structures in the western Corinth Rift (Greece). *Geophysical Journal International*, *215*(1), 196-221.

Dyer, B., R. Baria, et S. Michelet. 2004. « Soultz GPK3 stimulation and GPK3-GPK2 circulation May to July 2003 - Seismic monitoring report ». Report n° EEIG 05/2004. Semore Seismic for Socomine.

Ellsworth, W. L. (2013). Injection-induced earthquakes. *science*, *341*(6142), 1225942.

Fischer, T., & Hainzl, S. (2017). Effective stress drop of earthquake clusters. *Bulletin of the Seismological Society of America*, *107*(5), 2247-2257.

Fischer, T., & Hainzl, S. (2021). The growth of earthquake clusters. *Frontiers in Earth Science*, *9*, 79.

Gao, H., Schmidt, D. A., & Weldon, R. J. (2012). Scaling relationships of source parameters for slow slip events. *Bulletin of the Seismological Society of America*, *102*(1), 352-360.

Gerard, A., Baumgärtner, J., Baria, R., & Jung, R. (1997). An attempt towards a conceptual model derived from 1993−1996 hydraulic operations at Soultz. In Proceedings of NEDO International Symposium, Sendai, Japan (Vol. 2, pp. 329–341).

Glowacka, E., González, J. J., Nava, F. A., Farfan, F., & Diaz de Cossio, G., Monitoring surface deformations in the Mexicali valley, BC, Mexico Proceedings of tenth international symposium on deformation measurements (Vol. 175183) (2001)

Goebel, T. H., Hosseini, S. M., Cappa, F., Hauksson, E., Ampuero, J. P., Aminzadeh, F., & Saleeby, J. B. (2016). Wastewater disposal and earthquake swarm activity at the southern end of the Central Valley, California. *Geophysical Research Letters*, *43*(3), 1092-1099.

Goebel, T. H., & Brodsky, E. E. (2018). The spatial footprint of injection wells in a global compilation of induced earthquake sequences. *Science*, *361*(6405), 899-904.

Gualandi, A., Nichele, C., Serpelloni, E., Chiaraluce, L., Anderlini, L., Latorre, D., ... & Avouac, J. P. (2017). Aseismic deformation associated with an earthquake swarm in the northern Apennines (Italy). *Geophysical Research Letters*, *44*(15), 7706-7714.

Guglielmi, Y., Cappa, F., Avouac, J. P., Henry, P., & Elsworth, D. (2015). Seismicity triggered by fluid injection–induced aseismic slip. *Science*, *348*(6240), 1224-1226.

Hainzl, S., & Fischer, T. (2002). Indications for a successively triggered rupture growth underlying the 2000 earthquake swarm in Vogtland/NW Bohemia. *Journal of Geophysical Research: Solid Earth*, *107*(B12), ESE-5.

Hawthorne, J. C., & Rubin, A. M. (2013). Laterally propagating slow slip events in a rate and state friction model with a velocity-weakening to velocity-strengthening transition. *Journal of Geophysical Research: Solid Earth*, *118*(7), 3785-3808.

Hensch, M., Riedel, C., Reinhardt, J., Dahm, T., & The, N. I. C. E. (2008). Hypocenter migration of fluid-induced earthquake swarms in the Tjörnes Fracture Zone (North Iceland). *Tectonophysics*, *447*(1-4), 80-94.

Hirose, H., Matsuzawa, T., Kimura, T., & Kimura, H. (2014). The Boso slow slip events in 2007 and 2011 as a driving process for the accompanying earthquake swarm. *Geophysical Research Letters*, *41*(8), 2778-2785.

Houston, H., Delbridge, B. G., Wech, A. G., & Creager, K. C. (2011). Rapid tremor reversals in Cascadia generated by a weakened plate interface. *Nature Geoscience*, *4*(6), 404-409.

Ide, S., Beroza, G. C., Shelly, D. R., & Uchide, T. (2007). A scaling law for slow earthquakes. *Nature*, *447*(7140), 76-79.

Ito, Y., Obara, K., Shiomi, K., Sekine, S., & Hirose, H. (2007). Slow earthquakes coincident with episodic tremors and slow slip events. *Science*, *315*(5811), 503-506.

Jenatton, L., Guiguet, R., Thouvenot, F., & Daix, N. (2007). The 16,000-event 2003–2004 earthquake swarm in Ubaye (French Alps). *Journal of Geophysical Research: Solid Earth*, *112*(B11).

Keranen, K. M., Savage, H. M., Abers, G. A., & Cochran, E. S. (2013). Potentially induced earthquakes in Oklahoma, USA: Links between wastewater injection and the 2011 Mw 5.7 earthquake sequence. *Geology*, *41*(6), 699-702.

Keranen, K. M., & Weingarten, M. (2018). Induced seismicity. *Annual Review of Earth and Planetary Sciences*, *46*, 149-174.

Kraft, T., Wassermann, J., Schmedes, E., & Igel, H. (2006). Meteorological triggering of earthquake swarms at Mt. Hochstaufen, SE-Germany. *Tectonophysics*, *424*(3-4), 245-258.

Kim, W. Y. (2013). Induced seismicity associated with fluid injection into a deep well in Youngstown, Ohio. *Journal of Geophysical Research: Solid Earth*, *118*(7), 3506-3518.

Kwiatek, G., Saarno, T., Ader, T., Bluemle, F., Bohnhoff, M., Chendorain, M., ... & Wollin, C. (2019). Controlling fluid-induced seismicity during a 6.1-km-deep geothermal stimulation in Finland. *Science advances*, *5*(5), eaav7224.

Lambert, V., Lapusta, N., & Faulkner, D. (2021). Scale dependence of earthquake rupture prestress in models with enhanced weakening: implications for event statistics and inferences of fault stress. *Earth and Space Science Open Archive*, 55.

Larochelle, S., Lapusta, N., Ampuero, J. P., & Cappa, F. (2021). Constraining Fault Friction and Stability With Fluid-Injection Field Experiments. *Geophysical Research Letters*, e2020GL091188.

Lengliné, O., Lamourette, L., Vivin, L., Cuenot, N., & Schmittbuhl, J. (2014). Fluid-induced earthquakes with variable stress drop. *Journal of Geophysical Research: Solid Earth*, *119*(12), 8900-8913.

Lengliné, O., Boubacar, M., & Schmittbuhl, J. (2017). Seismicity related to the hydraulic stimulation of GRT1, Rittershoffen, France. *Geophysical Journal International*, *208*(3), 1704-1715

Lohman, R. B., & McGuire, J. J. (2007). Earthquake swarms driven by aseismic creep in the Salton Trough, California. *Journal of Geophysical Research: Solid Earth*, *112*(B4).

Madariaga, R. Dynamics of an expanding circular fault. *Bulletin of the Seismological Society of America*, *66*(3), 639-666 (1976)

Matsuzawa, T., Uchida, N., Igarashi, T., Okada, T., & Hasegawa, A. (2004). Repeating earthquakes and quasi-static slip on the plate boundary east off northern Honshu, Japan. *Earth, planets and space*, *56*(8), 803-811.

McGarr, A. (2014). Maximum magnitude earthquakes induced by fluid injection. *Journal of Geophysical Research: solid earth*, *119*(2), 1008-1019.

McGarr, A., & Barbour, A. J. (2018). Injection-induced moment release can also be aseismic. *Geophysical Research Letters*, *45*(11), 5344-5351.

Metois, M., Vigny, C., & Socquet, A. (2016). Interseismic coupling, megathrust earthquakes and seismic swarms along the Chilean subduction zone (38–18 S). *Pure and Applied Geophysics*, *173*(5), 1431-1449.

Montgomery-Brown, E. K., Shelly, D. R., & Hsieh, P. A. (2019). Snowmelt-triggered earthquake swarms at the margin of Long Valley Caldera, California. *Geophysical Research Letters*, *46*(7), 3698-3705.

Passarelli, L., Rivalta, E., Jónsson, S., Hensch, M., Metzger, S., Jakobsdóttir, S. S., ... & Dahm, T. (2018). Scaling and spatial complementarity of tectonic earthquake swarms. *Earth and Planetary Science Letters*, *482*, 62-70.

Passelègue, F. X., Almakari, M., Dublanchet, P., Barras, F., Fortin, J., & Violay, M. (2020). Initial effective stress controls the nature of earthquakes. *Nature communications*, *11*(1), 1-8.

Peng, Z., & Gomberg, J. (2010). An integrated perspective of the continuum between earthquakes and slow-slip phenomena. *Nature geoscience*, *3*(9), 599-607.

Raleigh, C. B., Healy, J. H., & Bredehoeft, J. D. (1976). An experiment in earthquake control at Rangely, Colorado. *Science*, *191*(4233), 1230-1237.

Roland, E., & McGuire, J. J. (2009). Earthquake swarms on transform faults. *Geophysical Journal International*, *178*(3), 1677-1690.

Roman, D. C., & Cashman, K. V. (2006). The origin of volcano-tectonic earthquake swarms. *Geology*, *34*(6), 457-460.

Ross, Z. E., Cochran, E. S., Trugman, D. T., & Smith, J. D. 3D fault architecture controls the dynamism of earthquake swarms. *Science*, *368*(6497), 1357-1361. (2020)

Rubin, A. M. (2008). Episodic slow slip events and rate-and-state friction. *Journal of Geophysical Research: Solid Earth*, *113*(B11).

Schmidt, D. A., & Gao, H. (2010). Source parameters and time-dependent slip distributions of slow slip events on the Cascadia subduction zone from 1998 to 2008. *Journal of Geophysical Research: Solid Earth*, *115*(B4).

Schultz, R., Atkinson, G., Eaton, D. W., Gu, Y. J., & Kao, H. (2018). Hydraulic fracturing volume is associated with induced earthquake productivity in the Duvernay play. *Science*, *359*(6373), 304-308.

Seeber, L., Armbruster, J. G., & Kim, W. Y. (2004). A fluid-injection-triggered earthquake sequence in Ashtabula, Ohio: Implications for seismogenesis in stable continental regions. *Bulletin of the Seismological Society of America*, *94*(1), 76-87.

Shapiro, S. A., Huenges, E., & Borm, G. (1997). Estimating the crust permeability from fluid-injection-induced seismic emission at the KTB site. *Geophysical Journal International*, *131*(2), F15-F18.

Shelly, D. R., Hill, D. P., Massin, F., Farrell, J., Smith, R. B., & Taira, T. A. (2013). A fluid-driven earthquake swarm on the margin of the Yellowstone caldera. *Journal of Geophysical Research: Solid Earth*, *118*(9), 4872-4886.

Skoumal, R. J., Brudzinski, M. R., & Currie, B. S. (2015). Distinguishing induced seismicity from natural seismicity in Ohio: Demonstrating the utility of waveform template matching. *Journal of Geophysical Research: Solid Earth*, *120*(9), 6284-6296.

Uchida, N. (2019). Detection of repeating earthquakes and their application in characterizing slow fault slip. *Progress in Earth and Planetary Science*, *6*(1), 1-21.

Wei, et al., The 2012 Brawley swarm triggered by injection-induced aseismic slip Earth and Planetary Science Letters 422, 115 (2015).

Wynants-Morel, N., Cappa, F., De Barros, L., & Ampuero, J. P. (2020). Stress perturbation from aseismic slip drives the seismic front during fluid injection in a permeable fault. *Journal of Geophysical Research: Solid Earth*, *125*(7), e2019JB019179.

Yoshida, K., & Hasegawa, A. (2018). Sendai-Okura earthquake swarm induced by the 2011 Tohoku-Oki earthquake in the stress shadow of NE Japan: Detailed fault structure and hypocenter migration. *Tectonophysics*, *733*, 132-147.

Zoback, M. D., & Gorelick, S. M. (2012). Earthquake triggering and large-scale geologic storage of carbon dioxide. *Proceedings of the National Academy of Sciences*, *109*(26), 10164-10168.

References from the Supporting Information

Albaric, J., Oye, V., Langet, N., Hasting, M., Lecomte, I., Iranpour, K., ... & Reid, P. (2014). Monitoring of induced seismicity during the first geothermal reservoir stimulation at Paralana, Australia. *Geothermics*, *52*, 120-131.

Baisch, S., Weidler, R., Vörös, R., Wyborn, D., & de Graaf, L. (2006). Induced seismicity during the stimulation of a geothermal HFR reservoir in the Cooper Basin, Australia. *Bulletin of the Seismological Society of America*, *96*(6), 2242-2256.

Baisch, Stefan and Rothert, Elmar and Stang, Henrik and Vörös, Robert and Koch, Christopher and McMahon, Andrew (2015) *Continued Geothermal Reservoir Stimulation Experiments in the Cooper Basin (Australia).* Bulletin of the Seismological Society of America, 105 (1). pp. 198-209

Bourouis, S., & Bernard, P. (2007). Evidence for coupled seismic and aseismic fault slip during water injection in the geothermal site of Soultz (France), and implications for seismogenic transients. *Geophysical Journal International*, *169*(2), 723-732.

Calò, M., & Dorbath, C. (2013). Different behaviours of the seismic velocity field at Soultz-sous-Forêts revealed by 4-D seismic tomography: case study of GPK3 and GPK2 injection tests. *Geophysical Journal International*, *194*(2), 1119-1137.

Cuenot, N., Dorbath, C., & Dorbath, L. (2008). Analysis of the microseismicity induced by fluid injections at the EGS site of Soultz-sous-Forêts (Alsace, France): implications for the characterization of the geothermal reservoir properties. *Pure and Applied Geophysics*, *165*(5), 797-828.

Daniel, G., et al. (2011), Changes in effective stress during the 2003–2004 Ubaye seismic swarm, France, *J. Geophys. Res.*, 116, B01309

De Barros, L., Baques, M., Godano, M., Helmstetter, A., Deschamps, A., Larroque, C., & Courboulex, F. (2019). Fluid-induced swarms and coseismic stress transfer: A dual process highlighted in the aftershock sequence of the 7 April 2014 earthquake (Ml 4.8, Ubaye, France). *Journal of Geophysical Research: Solid Earth*, *124*(4), 3918-3932.

De Barros, L., Cappa, F., Deschamps, A., & Dublanchet, P. (2020). Imbricated aseismic slip and fluid diffusion drive a seismic swarm in the Corinth Gulf, Greece. *Geophysical Research Letters*, *47*(9), e2020GL087142.

Duboeuf, L. (2018). *Injections de fluide dans une zone de faille (LSBB, Rustrel): sismicité induite et déformation asismique* (Doctoral dissertation, Université Côte d'Azur).

Duverger, C., Godano, M., Bernard, P., Lyon-Caen, H., & Lambotte, S. (2015). The 2003–2004 seismic swarm in the western Corinth rift: Evidence for a multiscale pore pressure diffusion process along a permeable fault system. *Geophysical Research Letters*, *42*(18), 7374-7382.

Duverger, C., Lambotte, S., Bernard, P., Lyon-Caen, H., Deschamps, A., & Nercessian, A. (2018). Dynamics of microseismicity and its relationship with the active structures in the western Corinth Rift (Greece). *Geophysical Journal International*, *215*(1), 196-221.

Dyer, B., R. Baria, et S. Michelet. 2004. « Soultz GPK3 stimulation and GPK3-GPK2 circulation May to July 2003 - Seismic monitoring report ». Report n° EEIG 05/2004. Semore Seismic for Socomine.

Edwards, B., & Douglas, J. (2014). Magnitude scaling of induced earthquakes. *Geothermics*, *52*, 132-139.

Fischer, T., & Hainzl, S. (2017). Effective stress drop of earthquake clusters. *Bulletin of the Seismological Society of America*, *107*(5), 2247-2257.

Gerard, A., Baumgärtner, J., Baria, R., & Jung, R. (1997). An attempt towards a conceptual model derived from 1993−1996 hydraulic operations at Soultz. In Proceedings of NEDO International Symposium, Sendai, Japan (Vol. 2, pp. 329–341).

Goertz-Allmann, B. P., Goertz, A., and Wiemer, S. (2011), Stress drop variations of induced earthquakes at the Basel geothermal site, *Geophys. Res. Lett.*, 38, L09308,

Hawthorne, J. C., Ampuero, J. P., & Simons, M. (2017). A method for calibration of the local magnitude scale based on relative spectral amplitudes, and application to the San Juan Bautista, California, area. *Bulletin of the Seismological Society of America*, *107*(1), 85-96.

Herrmann, M., Kraft, T., Tormann, T., Scarabello, L., & Wiemer, S. (2019). A consistent high-resolution catalog of induced seismicity in Basel based on matched filter detection and tailored post-processing. *Journal of Geophysical Research: Solid Earth*, *124*(8), 8449-8477.

Jenatton, L., Guiguet, R., Thouvenot, F., & Daix, N. (2007). The 16,000-event 2003–2004 earthquake swarm in Ubaye (French Alps). *Journal of Geophysical Research: Solid Earth*, *112*(B11).

Kim, W. Y. (2013). Induced seismicity associated with fluid injection into a deep well in Youngstown, Ohio. *Journal of Geophysical Research: Solid Earth*, *118*(7), 3506-3518.

Kwiatek, G., Saarno, T., Ader, T., Bluemle, F., Bohnhoff, M., Chendorain, M., ... & Wollin, C. (2019). Controlling fluid-induced seismicity during a 6.1-km-deep geothermal stimulation in Finland. *Science advances*, *5*(5), eaav7224.

Lengliné, O., Boubacar, M., & Schmittbuhl, J. (2017). Seismicity related to the hydraulic stimulation of GRT1, Rittershoffen, France. *Geophysical Journal International*, *208*(3), 1704-1715

Passarelli, L., Rivalta, E., Jónsson, S., Hensch, M., Metzger, S., Jakobsdóttir, S. S., ... & Dahm, T. (2018). Scaling and spatial complementarity of tectonic earthquake swarms. *Earth and Planetary Science Letters*, *482*, 62-70.

Ross, Z. E., Cochran, E. S., Trugman, D. T., & Smith, J. D. 3D fault architecture controls the dynamism of earthquake swarms. *Science*, *368*(6497), 1357-1361. (2020)

Seeber, L., Armbruster, J. G., & Kim, W. Y. (2004). A fluid-injection-triggered earthquake sequence in Ashtabula, Ohio: Implications for seismogenesis in stable continental regions. *Bulletin of the Seismological Society of America*, *94*(1), 76-87.

Yeck, W. L., Block, L. V., Wood, C. K., & King, V. M. (2015). Maximum magnitude estimations of induced earthquakes at Paradox Valley, Colorado, from cumulative injection volume and geometry of seismicity clusters. *Geophysical Journal International*, *200*(1), 322-336.

Yoshida, K., & Hasegawa, A. (2018). Sendai-Okura earthquake swarm induced by the 2011 Tohoku-Oki earthquake in the stress shadow of NE Japan: Detailed fault structure and hypocenter migration. *Tectonophysics*, *733*, 132-147.